THE STUDENT NITRIC OXIDE EXPLORER

S.C. Solomon, S.M. Bailey, T.E. Holden, D.C. O'Connor, J.P. Perich, M.A. Salada,
G.A. Stafford, K.R. Taylor, J.E. Vian, and P.R. Withnell
Laboratory for Atmospheric and Space Physics
The University of Colorado at Boulder
Boulder, Colorado 80309–0590
solomon@tethys.colorado.edu

1. Abstract

The Student Nitric Oxide Explorer (SNOE) is a small scientific spacecraft designed for launch on a Pegasus™ XL launch vehicle for the USRA Student Explorer Demonstration Initiative. Its scientific goals are to measure nitric oxide density in the lower thermosphere and analyze the energy inputs to that region from the sun and magnetosphere that create it and cause its abundance to vary dramatically. These inputs are energetic solar photons in the EUV and X-ray spectral regions, and energetic electrons that are accelerated into the polar regions, where they cause auroral disturbances and displays. Both of these phenomena are aspects of solar variability; thermospheric nitric oxide responds to that variability and in turn determines key temperature and compositional aspects of the thermosphere and ionosphere through its radiative and chemical properties.

The SNOE (*"snowy"*) spacecraft and its instrument complement is being designed, built, and operated entirely at the University of Colorado, Laboratory for Atmospheric and Space Physics (CU/LASP). The spacecraft is a compact hexagonal structure, 37" high and 39" across its widest dimension, weighing approximately 220 lbs. It will be launched into a circular orbit, 550±50 km altitude, at 97.5° inclination for sun-synchronous precession at 10:30–22:30 solar time. It will spin at 5 rpm with the spin axis normal to the orbit plane. It carries three instruments: An ultraviolet spectrometer to measure nitric oxide altitude profiles, a two-channel ultraviolet photometer to measure auroral emissions beneath the spacecraft, and a five-channel solar soft X-ray photometer.

The spacecraft structure is aluminum, with a center platform section for the instruments and primary components and truss work to hold the solar arrays. Power is regulated using switched arrays and a partial shunt. The attitude determination and control system uses a magnetometer, two torque rods, and two horizon crossing indicators to measure spin rate and orientation. Attitude control is implemented open-loop by ground commands. The command and data handling system is implemented using a single spacecraft microprocessor that handles all spacecraft and communications functions and instrument data. The communications system is NASA compatible for downlink using the Autonomous Ground Services station at Poker Flat; all mission operations, data processing, and analysis will be performed using a project operations control center (POCC) at the LASP Space Technology Research building.

2. Introduction

The Student Explorer Demonstration Initiative (STEDI) is a program administrated by the Universities Space Research Association (USRA) and funded by NASA. Its goal is to demonstrate that significant scientific and/or technology experiments can be accomplished with small satellites and constrained budgets. The original design parameters for low-earth-orbit experiments were "300 pounds to 300 nautical miles" for one year in polar or near-polar orbit. A firm budget limit of $4.3M was applied to the spacecraft, instruments, and all operations exclusive of communications services and the launch vehicle itself.

Following the enormous proposal response to the announcement of opportunity issued in Spring 1994, six experiments were selected for definition study. From these, two were chosen for flight, SNOE from the University of Colorado and the TERRIERS mission from Boston University. The CATSAT experiment from the University of New Hampshire was continued for further study. Meanwhile, NASA conducted a competitive process for selection of an ultralight expendable launch vehicle, which was won by Orbital Sciences Corporation. STEDI missions will fly on a Pegasus™ XL as one of two payloads, using approximately half of the launch capacity. Each STEDI mission will get its own launch, however, and will be the primary payload.

The SNOE mission is scheduled for launch in March 1997, leaving just two years for design and construction of the spacecraft and all systems. Meeting this tight schedule is the key to cost control on the project. A small leadership team, streamlined management, and minimal interference from the sponsoring agency are critical to the project's success. Collaboration with the Ball Aerospace Corporation and with the National Center for Atmospheric Research provides guidance to LASP engineering and management. Spacecraft system specialists from Ball serve as consultants to the project and two recently retired experts, John Simpson and Ron Brown, are now part-time employees at LASP. An additional collaboration with JPL provides a small technology experiment, the microGPS receiver for orbit determination.

Students are involved in all aspects of the project. Under the supervision of University and Industry mentors, they will build the spacecraft and instruments, write the flight software, integrate and test the instruments and subsystems, integrate with the launch vehicle, and operate the spacecraft. Advanced undergraduates and graduate students will analyze the data. The student training effort is coordinated through a course offered continuously in the CU Department of Aerospace Engineering Sciences by SNOE principal investigator Prof. Charles Barth.

2. Scientific Objectives

2.1 Objectives

Nitric oxide is an important minor constituent of the upper atmosphere that exhibits strong solar-terrestrial coupling. Nitric oxide directly affects the composition of the ionosphere, the thermal structure of the thermosphere, and may be transported downward into the mesosphere and stratosphere where it can react with ozone. However, significant unanswered questions about nitric oxide remain.

The scientific objectives of the Student Nitric Oxide Explorer are:

- to determine how variations in the solar soft X-radiation produce changes in the density of nitric oxide in the lower thermosphere, and
- to determine how auroral activity produces increased nitric oxide in the polar regions.

2.2 Background

Nitric oxide (NO) has a maximum density of about 3×10^7 cm^{-3} near 110 km (see Figure 1). In the polar region the mean density is several times greater and highly variable, sometimes as much as 10 times larger (see Figure 2). The importance of nitric oxide in the upper atmosphere is the result of its chemical, electrical, and radiative properties. Nitric oxide is more easily dissociated and ionized than the principal molecular constituents, nitrogen and oxygen. Nitric oxide radiates in the infrared while the major constituents of the atmosphere do not.

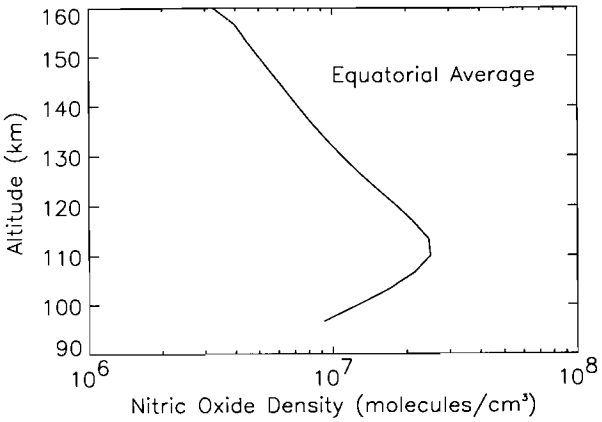

Figure 1. Nitric oxide density as a function of altitude. This profile is an average of SME observations in the equatorial region at times of low to moderate solar activity.

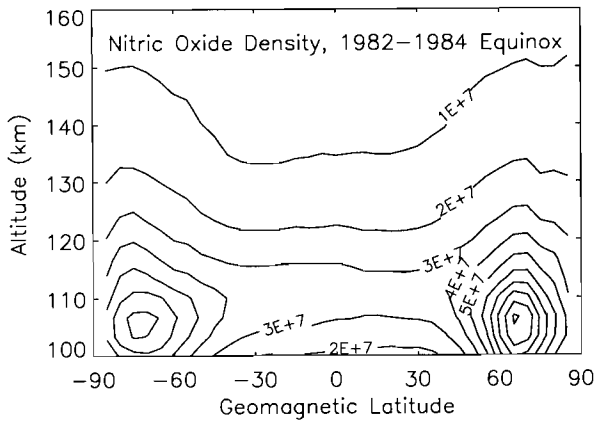

Figure 2. Latitudinal distribution of nitric oxide. Contour plot of the average nitric oxide density shows that the maximum density occurs in the auroral region.

Nitric oxide plays an important role in ionospheric chemistry at all latitudes, because the energy necessary to ionize it is less than the energy needed to ionize the major constituents, molecular nitrogen and atomic and molecular oxygen. Nitric oxide is a source of ionization in the D-region, the lowest region of the ionosphere. In the E and F1 regions of the ionosphere, nitric

oxide is an important participant in the ion-molecule and charge exchange reactions. Any change in the density of neutral nitric oxide produces changes in the composition and electron density of the ionosphere.

Nitric oxide plays an important role in the energy balance of the thermosphere. Since it is a heteronuclear molecule, it is able to radiate in the infrared portion of the spectrum, while molecular nitrogen and oxygen, being homonuclear molecules, are not. When nitric oxide density is high, its thermal emission at 5.3 μm makes a significant contribution to the cooling of the atmosphere.

Nitric oxide chemically reacts with ozone to form nitrogen dioxide which in turn reacts with atomic oxygen to reform nitric oxide. This is a catalytic cycle which destroys ozone while leaving the odd-nitrogen intact. Any nitric oxide that is transported downward from the lower thermosphere into the mesosphere and stratosphere may participate in the catalytic destruction of ozone. An opportune time for downward transport to take place is during polar night when photodissociation of nitric oxide does not occur [Solomon et al., 1982].

The principal source of nitric oxide in the lower thermosphere is the reaction of energetic nitrogen atoms with molecular oxygen. These nitrogen atoms need to have excess energy, either electronic or kinetic, in order for the reaction with molecular oxygen to proceed rapidly. Nitrogen atoms at normal temperatures in the lower thermosphere produce only a small amount of nitric oxide. Sources of the energetic nitrogen atoms are ionospheric reactions and energetic electron impact on molecular nitrogen. Energetic electrons created by photoionization (photoelectrons) and by auroral particle bombardment (auroral secondary electrons) thus create nitric oxide both by dissociating molecular nitrogen and by ionizing all neutral species, which drives ion-neutral and dissociative recombination reactions that create excited nitrogen atoms. While all of the solar extreme ultraviolet radiation (10.0–102.6 nm) and soft X-radiation (0.1–10 nm) produces ionization in the upper atmosphere, it is only the most energetic photons that are able to produce photoelectrons with sufficient energy to produce energetic nitrogen atoms from the dissociation of molecular nitrogen. For example, in the ionization of molecular nitrogen, a solar photon of wavelength 30.4 nm (41 eV) produces a photoelectron with sufficient energy (25 eV) to dissociate molecular nitrogen and produce an energetic nitrogen atom in the ^2D state (2.4 eV).

The hypothesis has been proposed that the variation in the density of low latitude nitric oxide at 110 km is caused by the variation in the solar output of soft X-rays in the wavelength range 2–10 nm [Siskind, et al., 1990]. The reasoning behind this hypothesis is that the absorption coefficients of the atmospheric constituents are such that the solar soft X-rays are absorbed in the 100–120 km altitude region and that the ionization by the soft X-rays produces a copious source of photoelectrons. The hypothesis further states that the solar soft X-rays vary with a greater amplitude than does the solar extreme ultraviolet radiation. The evidence for this hypothesis comes from three years of observations of thermospheric nitric oxide from the Solar Mesosphere Explorer [e.g., Barth, et al., 1988]. The SME observations show that the nitric oxide density at low latitudes varies with the 27-day solar rotation period and with the 11-year solar cycle. The variation of nitric oxide correlates with two solar indices, the solar Lyman alpha irradiance which was measured from the SME spacecraft and the solar 10.7 cm radio flux which is a solar index that is measured from the ground (see Figure 3). Neither of these emissions plays an actual role in the production of nitric oxide in the thermosphere—the correlation is due to the partial ability of Lyman alpha and the 10.7 cm flux to track solar EUV and soft X-rays. An examination of Figure 3 shows that the solar 10.7 cm flux is an imperfect index of the solar radiation that is causing the changes in nitric oxide density.

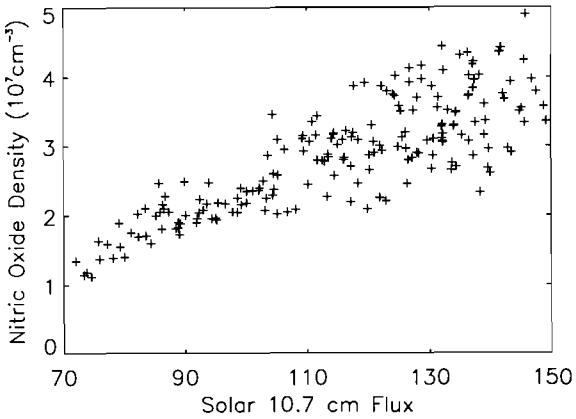

Figure 3. Variation of nitric oxide with solar activity. The nitric oxide density at 110 km is plotted as a function of the solar 10.7 cm flux which is an index of solar activity.

The first objective of the Student Nitric Oxide Explorer (SNOE) is to test this hypothesis. The solar soft X-ray irradiance in the wavelength range 2–10 nm and the solar extreme ultraviolet radiation between 10 and 31 nm will be measured with a solar X-ray photometer. The solar soft X-rays are expected to vary with a much larger amplitude than the 30.4 nm chromospheric line which is the most important extreme ultraviolet feature for ionization and photoelectron production. The nitric oxide density in the lower thermosphere will be measured with an ultraviolet spectrometer (215–237 nm) that observes the fluorescence of nitric oxide in the gamma bands. The comparison of the measured nitric oxide at low latitudes (25°S–25°N) between 100 and 120 km with the solar soft X-rays will show whether or not this hypothesis is correct. Further, the comparison of the observations will show the functional relationship between the magnitude of the nitric oxide density and the soft X-ray irradiance (2–10 nm) and the extreme ultraviolet radiation (10–31 nm). This functional relationship will be used to test and revise the photochemical model [Cleary, 1986; Siskind et al., 1990] to determine the relative roles of the various processes.

Global observations of nitric oxide from satellites have shown that the maximum amount of nitric oxide occurs in the polar regions centered at geomagnetic latitudes of 65°N and 65°S and in the altitude region between 100 and 110 km (see Figure 2). The most plausible explanation is that the polar region nitric oxide is produced by the impact of auroral electrons. When auroral primary electrons (energies 1–10 keV) bombard the atmosphere, they produce large numbers of secondary electrons. Those secondary electrons with energies greater than 13.3 eV are able to dissociate molecular nitrogen and produce energetic nitrogen atoms which in turn produce nitric oxide. Secondary electrons with energy greater than 15.5 eV ionize molecular nitrogen leading to the production of energetic nitrogen atoms. Photochemical theory indicates that any nitric oxide produced in the auroral zone will have a lifetime of greater than a day; thus, it is the auroral activity of the previous day or longer that should determine the amount of nitric oxide present. During the auroral bombardment process, the secondary electrons also excite molecular nitrogen and atomic oxygen to produce auroral emissions in the ultraviolet and visible portions of the spectrum. The intensity of these auroral emissions may be used to determine the flux of the auroral electrons. The theory of auroral excitation is well-developed [e.g., Solomon, 1993]. SME observations of nitric oxide in the polar regions show that there are large variations in nitric oxide density and that these variations are related to auroral activity [Barth, 1990; Barth, 1992]. Figure 4 shows average nitric oxide density profiles for conditions of low, medium, and high auroral activity. The geomagnetic index Ap was used to sort the observations into low, medium, and high activity; however, there is not a satisfactory quantitative relationship between nitric oxide density and the Ap index.

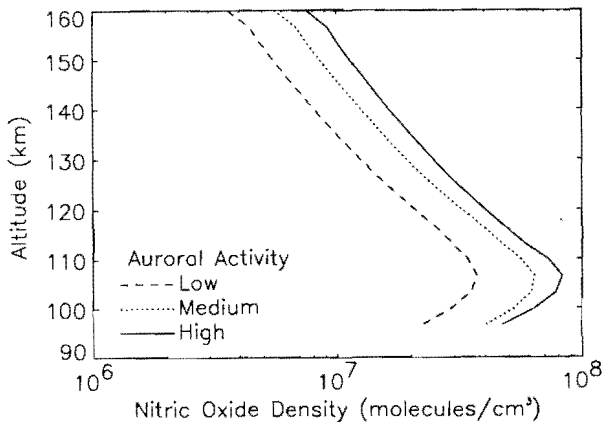

Figure 4. Nitric oxide density in the auroral region. SME observations show that nitric oxide density varies with auroral activity.

The second objective of SNOE is to determine how auroral activity produces increased nitric oxide in the auroral regions. This will be accomplished by measuring the nitric oxide density with the ultraviolet spectrometer and by measuring the intensity of the ultraviolet aurora with the auroral photometer. The auroral photometer will determine the intensity of the Lyman-Birge-Hopfield (LBH) bands of molecular nitrogen and the atomic oxygen resonance (130.4 nm) and forbidden (135.6 nm) lines, which are excited by auroral electron impact. Since the ultraviolet aurora will be measured on the nightside every orbit (96 min.) in both the north and south hemispheres, a global time history of auroral activity will be determined. The intensity of the auroral flux will be determined from the intensity of the LBH bands. The intensity of the atomic oxygen 130.4 nm line will be related to the auroral intensity through a radiative transfer calculation. The relationship between the auroral region nitric ox-

ide density and the time history of auroral intensity will be used to determine if in fact electron bombardment by auroral particles is the dominant process in producing polar nitric oxide.

3. Experimental Approach

3.1 Investigation Concept

The scientific objectives require the simultaneous observation of nitric oxide in the lower thermosphere, the solar irradiance in the soft X-ray region of the spectrum, and ultraviolet emissions from the auroral zone. All of these observations require remote sensing instruments. The nitric oxide measurement needs a limb-scanning telescope and ultraviolet spectrometer, the solar instrument needs to point at the sun and have some wavelength discrimination, and the auroral photometer needs to view in the nadir direction. These requirements lead to a spinning satellite in a low altitude orbit. Analysis of the nitric oxide photochemistry requires a sun-synchronous orbit with a local time of the daytime equatorial crossing between 9 AM and 3 PM. With the spin axis normal to the orbital plane, the ultraviolet spectrometer will scan through the limb of the earth in the orbital plane, the auroral photometer will scan through the nadir, and the solar photometers will scan through the sun on every satellite spin. The auroral intensity observation is best made between 22:30 and midnight. The simple design of the spinning satellite precludes an orbit near noon-midnight so that the earth viewing instruments do not view the sun during the satellite spin. Since the solar photometers have a field of view large enough to observe the sun from a 10:30–22:30 orbit this local time is chosen for the nominal orientation. A circular orbit with an altitude of 550±50 km is chosen to provide close viewing for the limb-scanning instrument and low enough atmospheric drag for at least one year of mission lifetime. The limb scanning ultraviolet spectrometer measures nitric oxide during the day, the auroral ultraviolet photometer observes in the nadir direction during both the day and night, and the solar photometer observes the sun when it is approximately overhead.

3.2 Experimental Method

The nitric oxide density will be determined by measuring gamma band fluorescent emissions with an ultraviolet spectrometer. The physical size and optical design of the instrument is the same as the SME ultraviolet spectrometer [Rusch et al., 1984]. The ultraviolet spectrometer will measure the (1,0) 215 nm and (0,1) 237 nm bands using the self-absorption technique demonstrated in the rocket experiment by Eparvier and Barth [1992]. Limb measurements will be made from 50 to 200 km with altitude resolution of 7 km by using the spinning motion of the satellite. The measurements below 70 km will be dominated by Rayleigh scattering from the neutral atmosphere, which will be used to calibrate the tangent ray height.

The design of the auroral photometer is based on the UV photometers that were developed for the Mariner 5 flight to Venus in 1967 [Barth et al., 1971]. Photometers of this type were also flown on OGO-5 and 6 [Thomas and Krassa, 1971]. Two photomultiplier tubes with cesium iodide photocathodes are used with calcium fluoride and barium fluoride filters to separate the atomic oxygen 130.4 nm line from the LBH bands and the atomic oxygen 135.6 nm line. The auroral photometer will detect auroral emissions over the polar regions during night; during daytime it will measure the far-ultraviolet dayglow.

The solar soft X-rays will be measured using photometers that have been developed at LASP and the NCAR High Altitude Observatory (HAO) for rocket experiments and EOS/SOLSTICE [Woods et al., 1994]. Thin metallic films are used to differentiate between various wavelength bands in the 1–31 nm range. These films of titanium, tin, aluminum, carbon, and scandium are directly deposited on silicon photodiodes.

4. Mission Design

4.1 Overview

The SNOE spacecraft is spin stabilized with the spin axis normal to the orbit plane. The orbit is circular at 550±50 km altitude and 97.5° inclination (sun synchronous). A 10:30–22:30 orbit is selected to meet the science and design requirements. The science requirements are described in subsection A.3.1, above; the design requirements are that the solar panels receive sufficient illumination but that the orbit is sufficiently far from the noon-midnight plane that it will not precess into it during the mission lifetime due to any launch vehicle injection errors. A sketch of the spacecraft (S/C) on orbit is shown below. A program lifetime on orbit of one year is anticipated. For the target altitude range, actual satellite lifetime should be significantly longer, which provides extra launch margin. Data requirements for comprehensive mission success are: measurements of nitric oxide altitude profiles, auroral energy flux along the satellite orbit, and solar X-ray emissions, for a period of at least 81 days (three solar rotations).

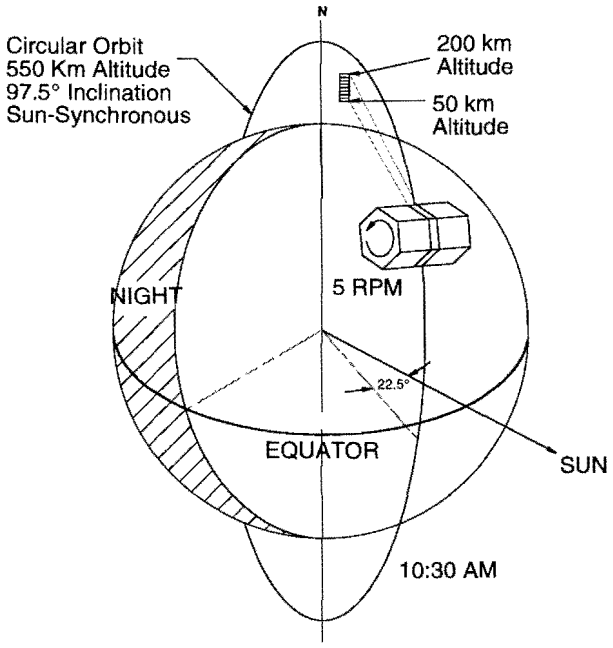

Figure 5. Mission scenario.

The SNOE spacecraft is a hexagonal aluminum structure, 37" high, and 39" across at its widest point. Total estimated weight is 206 lbs; with contingency, the total weight is 223 lbs. The mechanical subsystem provides the structural mounting platforms for the instruments, S/C engineering components, solar array and launch vehicle interface attach fitting. The instruments and primary S/C components are mounted on a solid platform in the center section. The outer two sections of the S/C are constructed of truss work to hold the twelve solar panels, antennas and launch vehicle attach fitting.

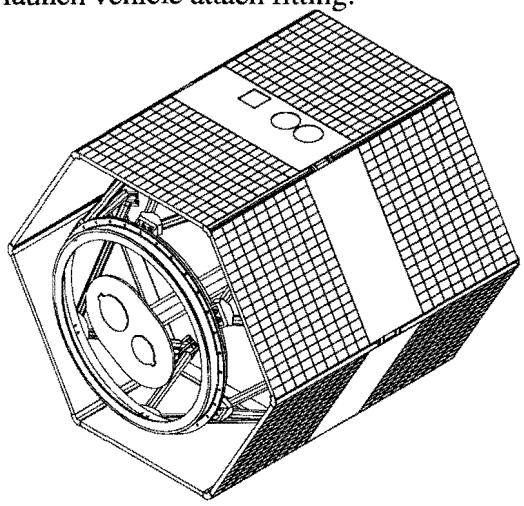

Figure 6. The SNOE spacecraft

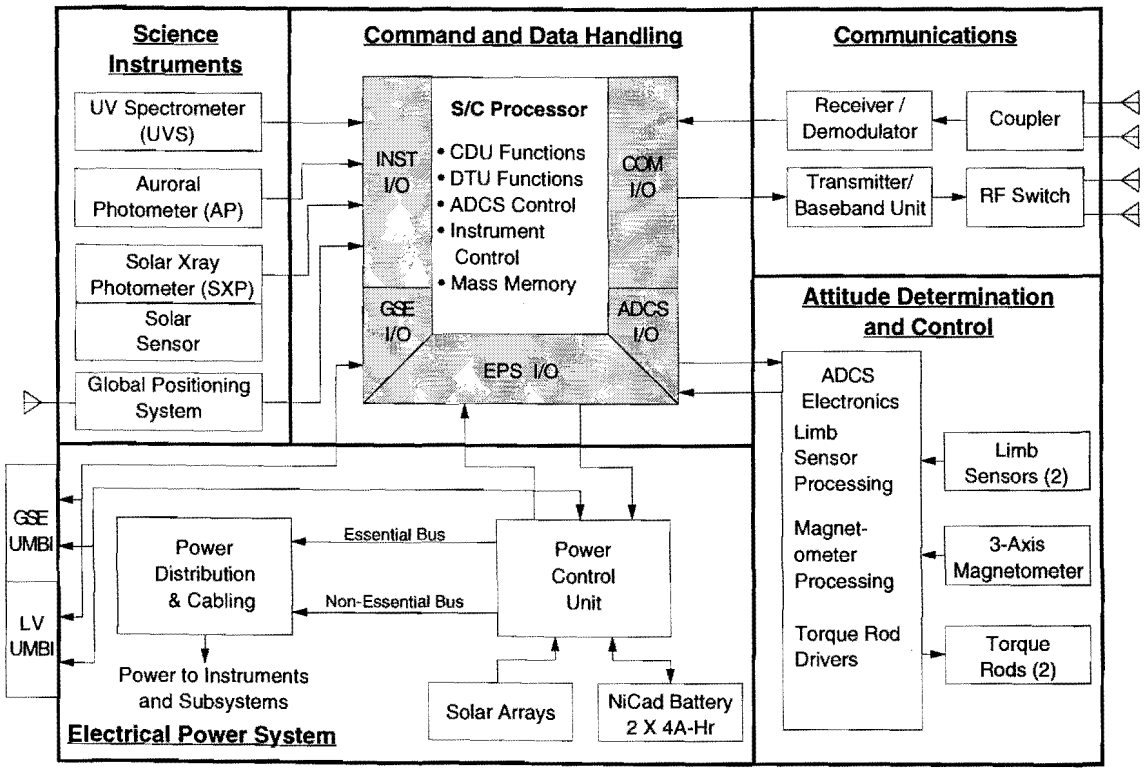

Figure 7. Spacecraft simplified block diagram

A simplified block diagram of the S/C electrical subsystems is shown in Figure 7. The power system is a direct energy transfer system using a combination of switched arrays and a partial shunt to provide unregulated D.C. power at 24 to 32 volts. The solar array consists of 24 strings of 76 cells each. The array produces 90 W at beginning of life (BOL) at an angle of incidence of 22.5°. Two batteries with 21 4-ampere-hour NiCd cells each are used to store energy. Battery charge is maintained by a voltage/temperature controlled shunt regulator and array switching using one of four voltage/temperature curves individually selected by ground command.

An open-loop Attitude Determination and Control System (ADCS) is used to keep the spin axis normal to the orbit plane within ±5°, maintain the spin rate at 5±1 rpm, and generate a limb reference pulse for the instruments. A magnetometer and two horizon crossing indicators are used for attitude determination. After determining the attitude and spin rate errors on the ground, stored commands are sent to the S/C, which are then issued when the magnetic field is at the proper angle to control the attitude and spin rate using precession and spin torque rods.

The Command and Data Handling system (C&DH) receives, decodes and distributes commands, formats digital and analog data, stores commands for later execution and stores data in a mass memory for downlink transmission. The system is based on a SwRI SC-4A microprocessor with a hardware decoder backup for critical commands. The realtime rate is 512 bps and the playback rate is 128 Kbps. The 8 Mbyte mass memory holds >24 hours of data, and is downlinked once per day. Realtime and playback data are Bi-Phase-Low (Bi-Φ_L) encoded.

The communications system uses a NASA compatible receiver/demodulator for the uplink and a transmitter/baseband unit for the downlink. Coupled microstrip patch antennas are used for the uplink and switched microstrip patch antennas are used for the downlink. Commands are uplinked at 2 Kbps. The 512 bps Bi-Φ_L realtime data is used to PSK modulate a 1.024 MHz subcarrier which in turn phase modulates the transmitter or is combined with the PBK data to phase modulate the transmitter.

4.2 Resource Budgets

The approach taken for the S/C and instrument design is to include both *contingency* and *margin* in weight and power calculations. Contingency is defined as the additional resource amount, estimated on a component basis, which may be needed to meet mission requirements. Margin is defined as the difference between the total estimate, including contingency, and the available resource.

Total estimated weight of the S/C is 206 lbs; total weight including contingency is 223 lbs. For a 97.5° sun-synchronous orbit, the launch vehicle specification translates into ~280 lbs to ~550 km altitude. Thus, the weight margin is ~57 lbs. Also, we have specified 550±50 km as an acceptable altitude range, since even a 500 km orbit will yield at least a one-year lifetime, which gives us additional launch margin.

Total estimated power required is 26 W; total power required including contingency is 29 W. To calculate the power margin, we need to allow for both solar panel degradation and for the possibility that injection errors could cause orbital precession to increase the solar angle of incidence. Assuming 20% degradation over the one-year mission, the solar arrays are designed to generate >47 W orbit average power at the nominal 22.5° solar angle. For a 30° solar angle, which corresponds to ~1-σ injection error, >44 W orbit average power would be generated, providing a margin of ~50%.

Table 1. Spacecraft weight and power budget summary

Subsystem	*Estimated Weight (lbs)*	*Contingency (lbs)*	*Total Weight (lbs)*	*Estimated Power (W)*	*Contingency (W)*	*Total Power (W)*
Instruments	19.2	2.9	22.1	5.5	0.8	6.3
ADCS	7.5	1.0	8.5	3.7	0.3	4.0
C&DH	5.0	0.3	5.3	7.0	0.3	7.3
Comm	12.0	0.2	12.2	4.4	0.0	4.4
EPS	38.4	3.2	41.6	5.0	1.3	6.3
Structure	78.4	4.7	83.1	0.0	0.0	0.0
Miscellaneous	46.0	4.7	50.7	0.7	0.0	0.7
S/C TOTALS	**206**	**17**	**223**	**26**	**3**	**29**

5. Spacecraft Structure

5.1 Structural Approach

The S/C structure consists a central mounting plate a launch adapter, two hexagonal solar arrays, and two antenna masts. The mounting plate supports the scientific instruments, S/C electronics, and equipment. These components attach to both sides of the mounting plate. Two patch antennas protrude slightly above the ends each solar array. Attached in a band to the periphery of the central support plate, between the solar arrays, are six thermal radiator plates. The plates have apertures for the instruments. Beta cloth and MLI cover the open hexagonal ends of the S/C when the assembly is complete. Metals used in the assembly are principally aluminum.

The first consideration in configuring the payload is to assure spin stability by designing the spin axis moment of inertia to be larger than the transverse axes moments of inertia. By careful distribution of components on the central plate and application of only 11 lbs of spin balance weights, the current configuration achieves a fully balanced S/C with a spin-to-transverse moment of inertia ratio of 1.14.

The assembled S/C fits within the dynamic envelope of a Pegasus™ XL launch vehicle with ample room for secondary payloads. The hexagonal structure is 39" maximum width and the overall S/C height is 37".

5.2 Spacecraft Structural Assembly

The S/C design involves four primary structural components: the central equipment and instrument mounting plate, two solar array assemblies and their support structures, the adapter structure that mates the S/C to the launch vehicle, including a separation assembly (marmon clamp and actuator), and two antenna masts. In addition to these elements there is a thermal control system that is described below. A drawing of the S/C configuration is shown in Figure 8.

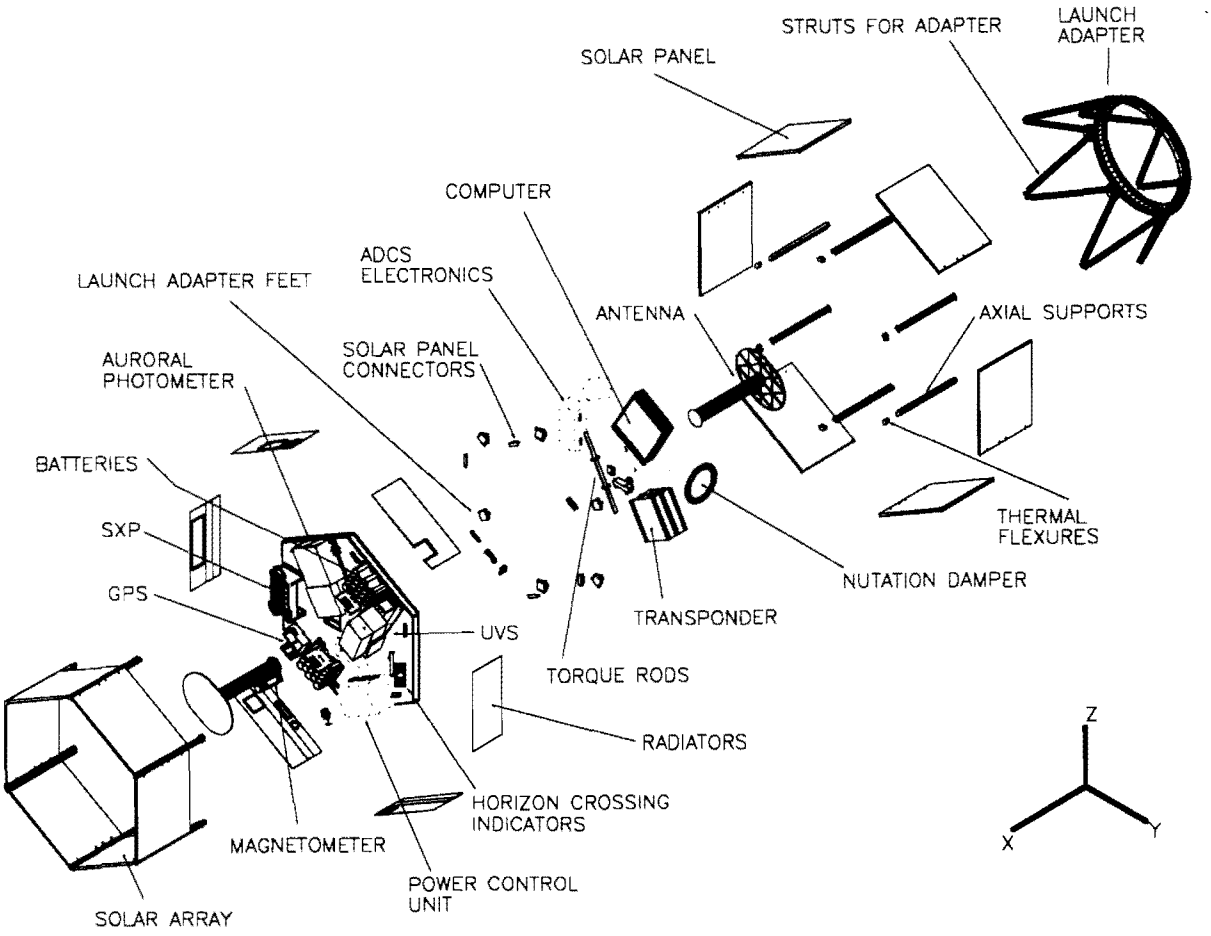

Figure 8. Spacecraft diagram

The central mounting plate provides support for the spacecraft electronics, instruments and cables. It firmly attaches to the adapter structure. It mounts both of the solar panel structures as well as the antenna assemblies. It provides a thermal path for heat generated in the interior of the spacecraft to reach the thermal radiators. The central mounting plate is fabricated from 1.5" thick aluminum honeycomb, using 0.05" thick face sheets. The edge close-outs consist of six aluminum square tubes 1" by 1.5", and six corner sections milled out of solid aluminum blocks 4" square by 1.5" thick. These corner sections provide additional strength to the corners of the central plate where the launch adapter struts attach.

The launch vehicle adapter structure mates the spacecraft to the launch vehicle. The assembly consists of twelve struts (1" diameter and .083" wall thickness) which connect the central plate to a 23.25" diameter marmon clamp on the launch vehicle end. The struts are attached to the marmon clamp and central plate in pairs through connection blocks machined out of aluminum. During integration the adapter structure will be attached to the launch vehicle marmon clamp using a clamp band.

The two hexagonal solar array assemblies consist of six 0.5" thick honeycomb panels that are approximately 18.75" wide by 13.5" tall. Solar cells are bonded to the surface of the honeycomb material using traditional mounting techniques. Two edges of each honeycomb panel attach to axial supports which serve as columns providing axial (spin axis) rigidity. Each set of six assembled solar arrays is a monocoque, using the panels as shear ties. The assembled structure joins to the spacecraft by bolting the axial supports to thermal flexures which in turn are bolted to the central mounting plate. The thermal flexures consist of a thin (0.1") "blade" of titanium 1.0" in length. This approach allows the spacecraft equipment to be managed thermally without concern for the varying solar panel temperatures. The construction of the top and bottom solar array structures is essentially identical. Each end of the spacecraft requires a closeout of MLI blanket and Beta cloth. On the bottom end the spacecraft adapter structure will provide the necessary support for this material; on the top end of the structure a "spider" provides the necessary tie downs and fastening locations.

There are two patch antennas located on the spin axis at each end of the spacecraft. The antennas consist of a support tube and a thin plate. This assembly mounts to each side of the central mounting plate. The column provides structural support for the antenna, and precisely positions it so that the ground plane of the antenna sits above the solar panel.

5.4 Structural Analysis

A finite element model of the spacecraft structure was constructed using Cosmos/M. The model consists 2278 elements and 1652 nodes. Modal analysis for the first ten modes were analyzed, and simulations were run to determine mode response and displacements. The structural model includes the adapter structure, the mounting plate and solar arrays. Masses representing most of the spacecraft electrical and sensor components, as well as the spacecraft instruments, were also included. The first mode frequency is 56 Hz, corresponding to a cantilever mode off the launch adapter marmon clamp assembly.

6. Scientific Instruments

Instrumentation for the SNOE mission consists of an ultraviolet spectrometer to measure nitric oxide density, a solar soft X-ray photometer to measure the solar irradiance at wavelengths from 2 to 31 nm, and an auroral photometer to measure the flux of energetic electrons entering the Earth's atmosphere at high latitude. A small GPS receiver will also be carried as a technology experiment. A companion paper by Bailey et al. describes the instruments in more detail; they are briefly summarized below.

6.1 Ultraviolet Spectrometer

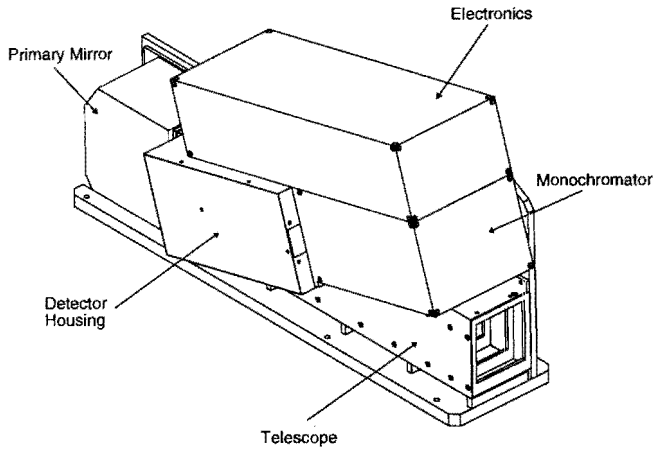

Figure 9. Ultraviolet spectrometer.

The primary function of the ultraviolet spectrometer (UVS) is to measure the densities of nitric oxide between the altitudes of 50 and 200 km

in the terrestrial upper atmosphere by observing the (1,0) and (0,1) gamma bands. The UVS design was developed under the SME program and was successfully flown on SME. It consists of an Ebert-Fastie spectrometer, an off-axis telescope, and two Hamamatsu phototube detectors. The spectrometer has a focal length of 125 mm and uses a 3600 l/mm mechanically ruled plane grating which produces a dispersion of 2.15 nm/mm at the detectors. The phototubes each have fused silica windows and a cesium telluride photocathode. The telescope is an off-axis parabola with a 250 mm focal length. The UVS is mounted with its optical axis perpendicular to the spin axis of the S/C. Its telescope images the entrance slit of the spectrometer on the limb with the long axis of the slit parallel to the horizon. The image of the slit on the limb is 7 km high, which determines the fundamental altitude resolution of the instrument. The integration time of the is set to 28 milliseconds for 2× spatial oversampling. Once the S/C has achieved orbit, the UVS high voltage will be turned on and each channel will produce a continuous stream of data. To minimize requirements on the S/C, data will only be stored for the downward limb scan. The data are stored in a buffer which will be periodically emptied, time-tagged, and stored by the S/C microprocessor.

6.2 Auroral Photometer

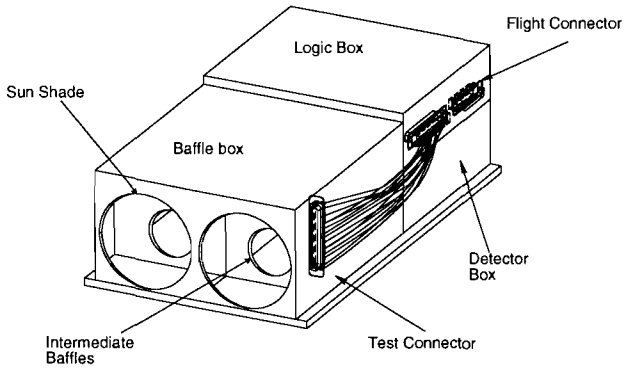

Figure 10. Auroral photometer

The auroral photometer (AP) is a two-channel broad-band instrument that will be used to determine the energy deposited in the upper atmosphere by energetic auroral electrons. The channels consist of two Hamamatsu phototube detectors, a UV window/filter for each channel, and a field of view limiter for each channel. Both channels have circular fields of view, 11° full-cone. The detectors are identical phototubes with magnesium fluoride (MgF_2) windows and cesium iodide (CsI) photocathodes. Channel A has a calcium fluoride (CaF_2) filter placed in front of the detector and channel B has a barium fluoride (BaF_2) filter. The combination of the CsI photocathode and the CaF_2 filter produces a bandpass from 125 to 180 nm for channel A, allowing a combined measurement of the LBH bands, the OI doublet at 135.6 nm, and the OI triplet at 130.4 nm. Channel B has a 135 to 180 nm bandpass, providing a measurement of the LBH bands and the OI doublet at 135.6 nm with the exclusion of the OI triplet at 130.4 nm. The AP and UVS photomultiplier electronics are identical, resulting in significant economies in fabrication and operation. As with the UVS, the AP is mounted with its optical axis perpendicular to the S/C spin axis. The AP produces continuous data but at a much lower rate than the UVS. Only the downward-looking 180° of each spin (limb-to-limb nadir scan) will be stored.

6.3 Solar X-Ray Photometer

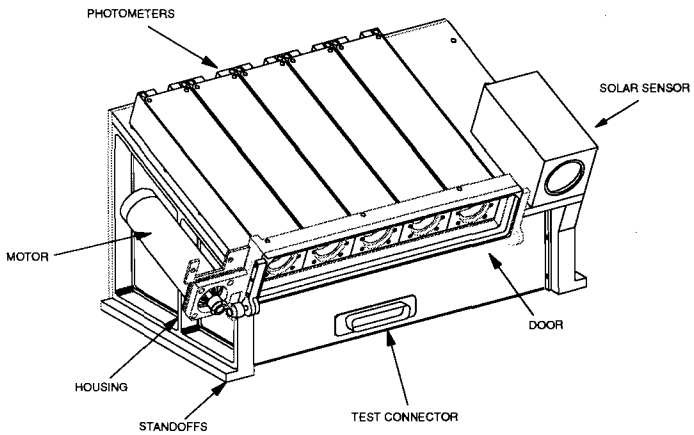

Figure 11. Solar X-ray photometer

The solar X-ray photometer (SXP) measures the solar irradiance at wavelengths from 2 to 31 nm. Each of the five photometer channels contains a silicon photodiode; wavelength selection is accomplished by thin metallic films deposited directly onto the diode surface. Coatings are selected so that overlapping bandpasses can be used to isolate key parts of the solar soft X-ray and hard EUV (or "XUV") spectrum at low resolution. The fields of view are ~70° full-cone to obtain a solar measurement once per spin during the day. Each photodiode is followed by a current amplifier and a voltage-to-frequency converter, resulting in a sequence of pulses with a frequency proportional to the diode current. Part of the measured current is due to visible-wavelength radiation entering through micro-

scopic flaws in the coating. To measure these background currents a door mechanism fitted with a fused silica window is included. The fused silica allows all visible light to reach the photodiode but rejects light below 160 nm, thus when the door is closed the signal is completely due to background visible light. The window is opened and closed periodically, and the X-ray signal obtained by subtracting data taken with the window closed from data taken with the window open. A small two-axis sun sensor is co-aligned with the SXP to measure the solar incidence angle for the instrument, since the measured signal will vary as the cosine of this angle. Instruments of this design have flown on LASP and HAO sounding rockets five times [Woods et al., 1994] and are scheduled for four more flights during 1995–96.

6.4 GPS Receiver

A small GPS receiver for orbit determination is included on SNOE as a technology experiment. This instrument, the JPL microGPS "bit-grabber", is the result of a collaboration between JPL, NASA Code O, the CU Aerospace Sciences Engineering department, and LASP. The microGPS electronics box is approximately 2.5" × 4.5" × 2.0" and a small integral antenna views through a radiator aperture as do the other instruments. Estimated mass is 1.5 lbs. Power consumption is 2.1 W while operating, but orbit average power is reduced to about 0.02 W by extreme duty-cycling. This is the essence of the microGPS approach—the receiver turns on for a few seconds, samples available signal from the GPS constellation, and then goes back into "sleep" mode. It does this three times per orbit, which is the minimum number necessary to fully specify the orbit. The signal is not processed on board but is stored in S/C memory until the next downlink. Data processing and orbital determination is then done after-the-fact on the ground. Thus, the microGPS is not relied upon for orbit tracking (which will be accomplished using NORAD updates) and is considered as part of the instrument experiment complement rather than a S/C subsystem.

7. Electrical Power and Distribution

The Electrical Power System (EPS) generates energy, stores energy for use during peak demand cycles (e.g., during transmitter operation) and during orbit eclipse and controls the distribution of energy to the required S/C and payload systems. Figure 12 is a simplified functional block diagram of the EPS. This figure shows the primary EPS functional elements as well as the monitoring and switching circuits used in the generation and control of S/C power.

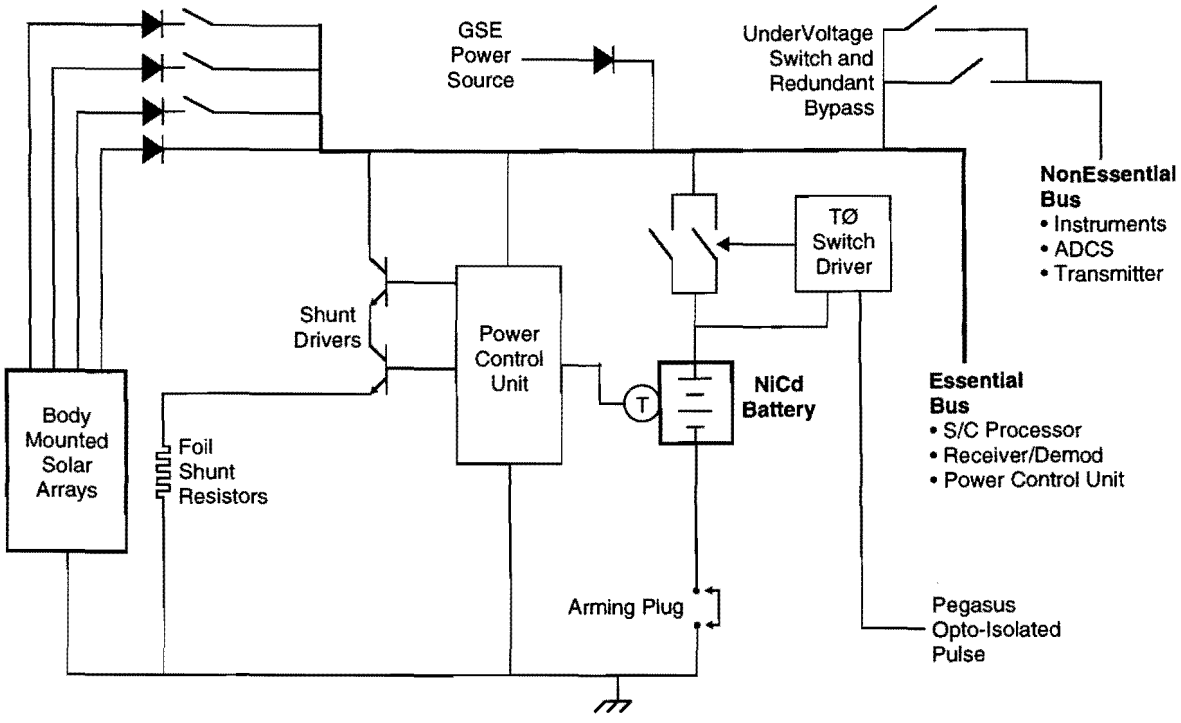

Figure 12. Electrical power system block diagram

Power is generated by body mounted panels of solar arrays. There are twelve rectangular panels, each containing 2 array circuits (strings) for total of 24 strings. The strings consist of seventy-six 2.3 cm x 4.1 cm silicon photovoltaic cells. Diode isolation of the individual array circuits from the bus is used to prevent a failure in an array string from causing a failure of the entire power generation system. Assuming one-year degradation of 20% and a 30° solar angle of incidence, the solar arrays will generate >44 watt orbit average power at EOL, providing a >50% margin.

The solar cells are purchased from Heliokinetics of Palm Springs, CA. The 10 Ω-cm, 8 mil thick cells are AR coated and delivered with pre-installed cover glass and interconnection butterfly fittings. Criteria and procedures for selection of the individual flight solar cells include testing for cell open circuit voltage and short circuit current. Assembly of the arrays will be performed by student assemblers at LASP.

Energy required for peak loads and during the eclipse portion of the orbit is stored in two 21-cell 4-Amp-hour Nickel Cadmium (NiCd) battery packs. The batteries use Sanyo N cells, tested, integrated and qualified by a flight proven Ball Aerospace process. The power usage profile produces an average battery depth of discharge of ~7%. Only one battery is necessary for operation but two are provided for redundancy; a one-time relay can be thrown to remove one battery from operation if it fails.

A shunt regulator is used to prevent overcharging of the battery and the associated generation of excess heat. Shunt regulation is performed by clamping the bus voltage to a level set by predetermined voltage and temperature curves (V-T control). Bus clamping action (regulation) is implemented by a two mode shunt controller which uses a combination of conventional linear shunt regulation (fine control mode) along with solar array string switching (coarse control mode).

The coarse control is achieved using switched array strings controlled by the V-T controller in a closed loop fashion. There are four switching circuits of six strings each, with the six strings distributed one to each S/C face to prevent current fluctuation when one or two circuits are switched off. Fine control is performed by a linear regulator that shunts excess power into resistors mounted on the inside of the solar panels. The V-T controller uses 4 temperature voltage curves selected by uplink command. Power distribution includes two primary power busses; the essential bus and the non-essential bus. Circuits on the essential bus are the EPS itself, the command receiver/demodulator, and the S/C processor. All other loads are considered non-essential and are therefore disconnected when the bus voltage monitor detects a low voltage condition.

8. Communications Subsystem

The NASA compatible communications subsystem, consisting of a receiver / demodulator, transmitter / baseband unit, hemispherical antennas, coupler, RF switch, and filter, provides a traditional yet low-cost approach. The transmitter and receiver are purchased from Cincinnati Electronics. The 2 Kbps NRZ-M command data is transmitted using NASA compatible PCM/PSK/PM modulation. The realtime telemetry modulation is PCM/PSK/PM, and the playback is PCM/PM.

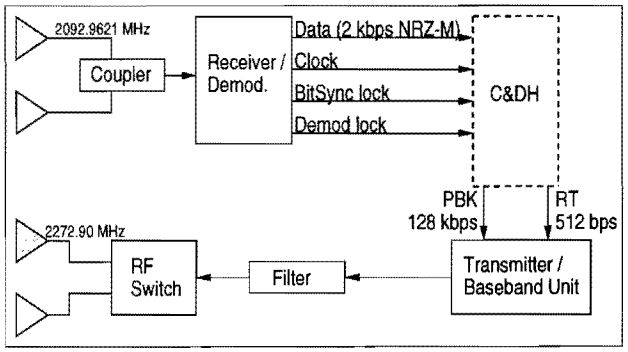

Figure 13. Communication system simplified block diagram

The receiver, fixed tuned to the assigned frequency at 2093 MHz, features a double conversion technique that eliminates EMI generating multiplier circuitry and uses a single local oscillator to reduce costs, power consumption and parts count. The receiver acquisition threshold is -124 dbm and the command sensitivity is -115 dbm at a BER of 1 x 10^{-6}. The demodulation is performed directly at the 16 KHz subcarrier through implementation of a modified costas loop.

The transmitter/baseband unit provides 5 watts of output RF power. The unit accepts the 512 bps Bi-$\emptyset_L$ realtime data and PSK modulates a 1.024 MHz subcarrier. The baseband unit either phase modulates the transmitter with the subcarrier or combines the subcarrier with the 128 Kbps Bi-$\emptyset_L$ playback data and then phase modulates the transmitter. The power amplifier

uses GaAs FET power devices operating as a class AB amplifier to reduce generation of spurious signals.

Each antenna assembly consists of wide-beam command and wide-beam telemetry radiating elements mounted on a common ground plane. The radiating element is a 1/2 wavelength disc etched by chemically removing some of the copper cladding on the upper surface of the copper-clad Teflon-impregnated fiberglass cloth. Right-hand circular polarization is achieved by positioning the feed point on the radiating element. The command antennas are coupled to provide omnidirectional coverage; the telemetry antennas are selected through the RF switch to improve the link margin while reducing the interferometer effect

Command uplink and telemetry downlink margins are large: 8 db for command uplink, 15 db for realtime telemetry downlink, and 7 db for playback telemetry downlink, assuming use of a 4 meter AGS antenna. Margins are much larger if the 11 meter antenna at Wallops Island is used in a contingency situation.

9. Attitude Determination and Control

SNOE is a passive spin-stabilized spacecraft that uses an open-loop attitude determination and control system (ADCS) to keep the spin axis normal to the orbit plane, limit nutation, maintain a stable spin period, and generate payload timing signals. Attitude determination is accomplished using two horizon crossing indicators (HCI) in a V-pair configuration. Two electromagnets (torque rods), one aligned with the spin axis (y-axis) and a second normal to the spin axis (z-axis) are used to correct S/C alignment and spin rate. Quarter-orbit torquing is performed open-loop using stored command sequences which are uplinked from the POCC. Spin rate is also adjusted by ground command. A spin magnetometer measures magnetic field orientation relative to the z-axis so that the z-axis torque rod can be modulated to alter spin rate. The favorable spin/transverse moment of inertia ratio (1.14) and a ring nutation damper cause the S/C to have intrinsic spin stability; once the S/C y-axis is aligned with the orbit normal, only occasional adjustment of the spin rate and ~1 °/day spin axis torquing to adjust for orbital precession will be required.

In addition to providing attitude information, the attitude sensors also generate timing signals for use by the science payload. The HCI limb pulses initialize timer circuits that enable data taking during the appropriate portion of the S/C spin period. The limb crossing measurement obtained from the HCI will be better than 1° precision, but that is not sufficient for accurate analysis of the nitric oxide density profiles. Therefore, Rayleigh scattered sunlight from the atmosphere measured on the limb by the UVS will be used to calibrate after-the-fact limb timing knowledge; this technique was used effectively on SME.

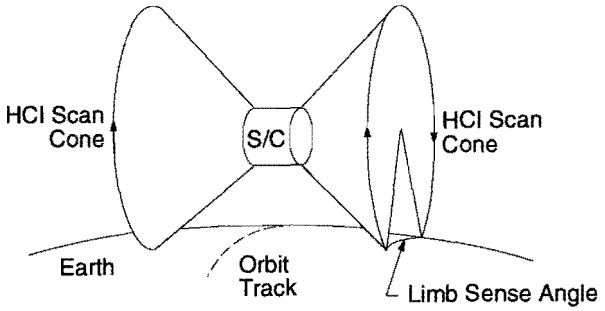

Figure 14. Method for determining spacecraft roll errors using two horizon crossing indicators.

Further description of the ADCS approach may be found in a companion paper by Holden and Lawrence.

10. Command and Data Handling

10.1 C&DH Requirements

The command and data handling system provides the commanding functions traditionally implemented by a command decoder unit (CDU), the telemetry collection and formatting functions usually found in a digital telemetry unit (DTU), command memory storage, mass memory for TM data storage, and the encoding and conditioning circuitry.

The requirements for CDU functions are the ability to verify NASA/GN formatted commands, to decode and verify the correct S/C address, decoder address, parity, and message length, to route the validated commands in real time to their proper address, and to execute stored sequence commands. The requirements for DTU functions are to accept bi-level, analog, and serial digital telemetry from multiple sources, to format these into packets and output the packets in a single serial data stream, to include in the frame the vehicle time code word and frame synchronization words, to provide timing and frame synchronization signals to the remainder of the S/C, and to output the frames in real time at a rate of 512 bps Bi-$\emptyset_L$ to the communication subsystem. The command memory requirements are very minimal. A minimum set of stored sequence com-

mands have been identified, such as transmitter on/off commands, post-launch configuration commands, and torque commands. To accommodate these and other possible requirements with large contingency, we have allocated 32 Kbytes of memory for stored commands. The mass memory requirements are also relatively minimal. Based upon the science requirements, we have defined a maximum requirement of 6 Mbytes per day of data storage. Because of this small requirement, we will use solid state memory for the S/C data storage.

10.2 Spacecraft Processor

A Southwest Research Institute (SwRI) SC4A microprocessor has been selected as the S/C processor. The SC-4A includes an Intel 80C186 CPU, watchdog timer and other programmable timers, interrupt controller, serial ports, at least 8 MByte of mass storage, 64 Kbyte of EPROM, 256 Kbytes of EEPROM, 256 Kbytes of RAM (all memory includes single bit correction, double bit detection error detection and correction (EDAC)), 32 channel analog-to-digital converter, 8 channel digital-to-analog conversion, multiple digital I/O ports, an expansion buffer for a daughter board, and four separate current monitored power lines in order to protect the unit from catastrophic damage due to latch-up.

Functions that otherwise would have required external subsystems are integrated into the SC-4A, including the CDU, DTU, MMU, and attitude determination functions. The MMU was replaced by the 8 Mbyte internal mass memory in the SC-4A since we require only ~6 MByte of mass memory storage, and data integrity should remain good due to the SC-4A error correction circuitry. The DTU is replaced using a daughter board containing only I/O circuitry. A ROM-based lookup table combines the TM channel data into frames in real time.

CDU functions are implemented through a combination of hardware and software. Command verification, checking, and decoding occurs in software, and simple hardware output ports and appropriate driver circuitry are used to issue serial digital and discrete commands (both low and high level) to the remainder of the S/C. Stored sequence commands will be stored within the S/C processor memory, and will be executed based upon the internal S/C Processor real time clock.

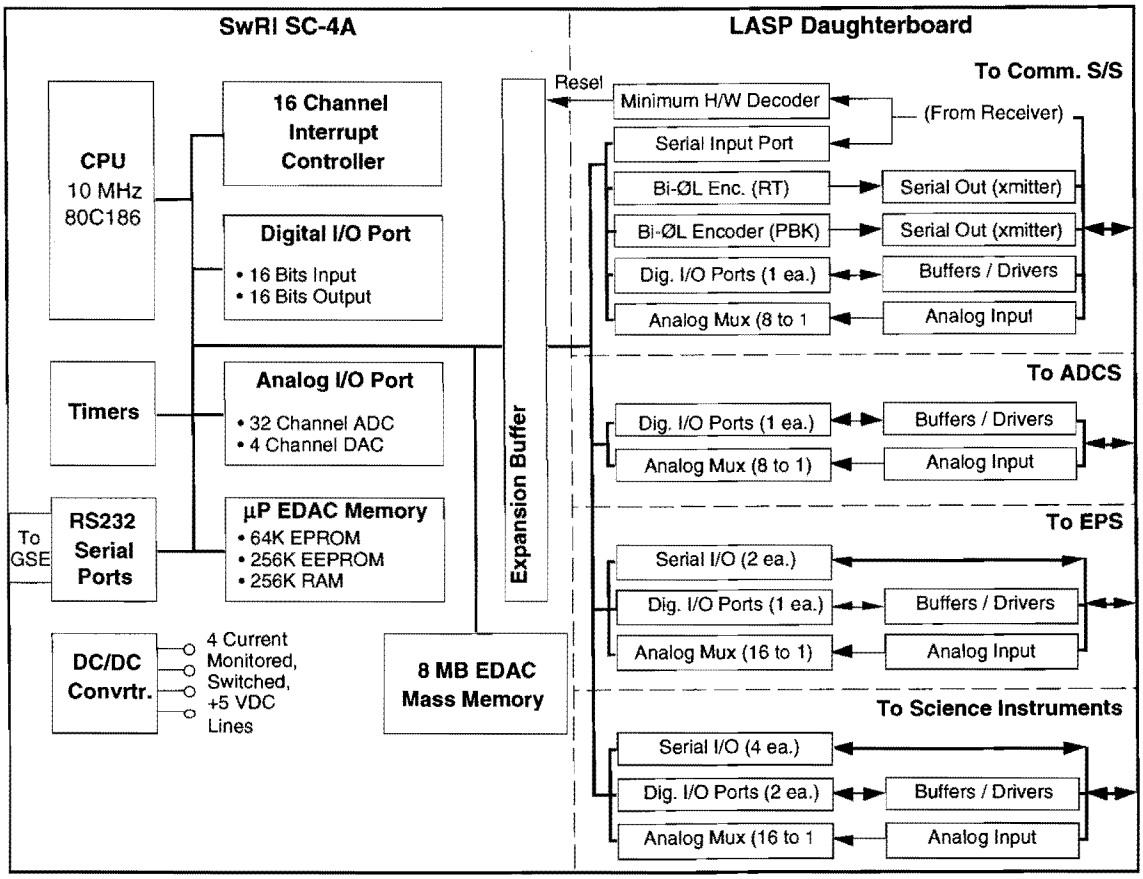

Figure 15. Spacecraft Processor block diagram

A small hardware decoder is also provided that can reset the SC-4A by ground instruction. This is included to give command access in case the SC-4A ever fails to automatically reset. Bi-$\emptyset_L$ encoding is also be done in hardware.

In addition to the functions listed above, the SC-4A acts as the instrument controller. The instruments require few interactions with the CPU, mostly for science data collection and storage.

10.3 Flight Software

Flight software and telemetry design and implementation is described in a companion paper by Salada and Davis.

11. Thermal Control

The SNOE thermal design consists of multilayer insulation (MLI) blankets, passive radiators, and conductive isolation. Electrical heaters for each battery and at selected baseplate locations are included for contingency operation in case part of the S/C runs too cold. The basic design concept is shown in Figure 16. The solar panels are kept thermally isolated from the central plate as described above in section 5 so that they may fluctuate in temperature while the subsystems and instruments remain fairly stable. This design has been analyzed using the SINDA-85 and TRASYS mathematical models. Sample results for a nominal orbit case are shown in Figure 17.

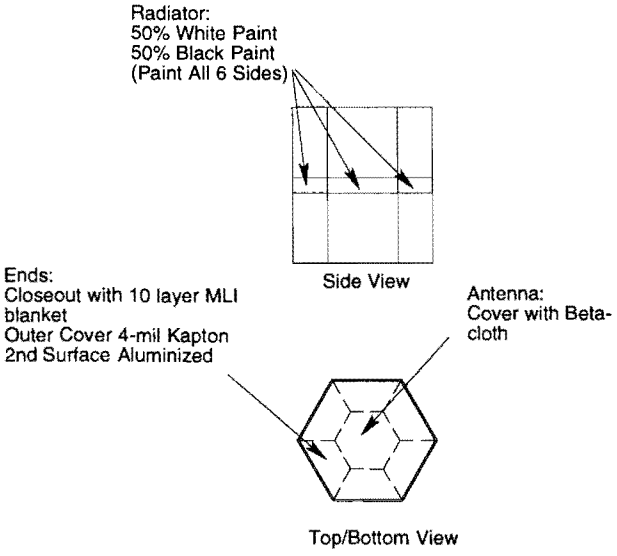

Figure 16. Thermal control concept

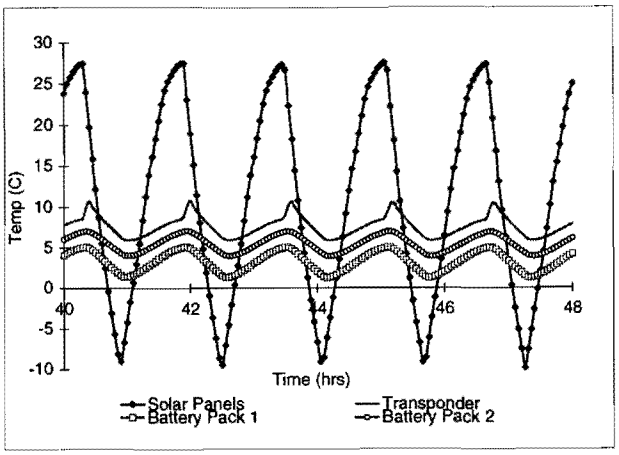

Figure 17. Thermal modeling results.

12. Integration and Test

Integration and test of the SNOE S/C will be performed at facilities at the LASP Space Technology Research Building and at Ball Aerospace in Boulder. Final integration of the instruments and subsystem components with the S/C will be done in a large class-100,000 clean room located at LASP.

A comprehensive protoflight component test program will be used to ensure the instruments and S/C engineering components meet their performance requirements over the expected environmental conditions. All components will be designed to meet MIL-STD-461 to ensure compatibility. EMI testing is planned only for the S/C computer at this time. Pyro shock testing will be deferred and conducted as part of the S/C separation test. Thermal vacuum testing will be performed on all high voltage or high power dissipating components. Acoustic testing is not planned for any components at this time.

After structural final assembly, acceleration load testing, and fit checks, the harness and will be installed and checked pin for pin with the wire list. S/C subsystems will be installed and limited functional testing performed after initial power, ground and isolation checks are made using breakout boxes. A full S/C functional test will be performed prior to the start of instrument integration. Compatibility testing will be performed prior to the start of instrument integration using a NASA ground network van. Instruments will then be integrated one at a time, similar to the S/C subsystems. The instruments will be individually functionally tested after initial checks through the breakout boxes. Then full S/C functional test will be performed including the instruments.

The primary system level tests include functional tests, alignments and integrated system tests. The functional test is a fully automated command/response test using only external stimulus. All S/C subsystem and instrument commands are sent and the responses verified via telemetry. The tests are run using the test computer which automatically steps through the procedure, verifies that each response is within limits, and stops the procedure if an out-of-limit condition is found. Alignment tests check that instrument and HCI alignments have not shifted out of tolerance following environmental exposures. The S/C alignment cube is initially referenced to the S/C axes using a surface table and a theodolite. The integrated system test is performed prior to environmental testing to establish a baseline and after all the environmental tests to ensure no degradation has occurred. It includes a full functional, special performance tests, alignments and orbit simulations.

The planned environmental tests for SNOE include EMC, separation/shock, random vibration, thermal vacuum, and mass properties. The EMC test planned for SNOE will include a self compatibility test and radiated susceptibility test. The self compatibility test is conducted by placing each S/C component and instrument in their most sensitive mode one at a time while exercising all other components and instruments in their most noisy mode. The test is run via an RF link to ensure the EGSE does not influence the test results. The radiated susceptibility test will be performed in the launch mode with the S/C being radiated with expected launch tower environments. The separation/shock test is conducted in the cleanroom without special instrumentation to ensure the shock from the pyros and marmon clamp separation do not cause a failure. The pass/fail criteria will be the successful completion of a functional test after exposure to the shock. The S/C will be subjected to protoflight level random vibration testing. Limited functional tests will be run prior to and after exposure to ensure S/C health. The S/C will be placed in launch configuration for the test. The thermal vacuum test will be conducted using the chamber shroud to control the component temperatures. We plan to complete four thermal cycles during the test. High and low voltage functional tests will be performed at the temperature extremes. Weight and CG measurements will be performed in the cleanroom. The S/C will be spin balanced and additional balance weights added as required. A limited magnetic balance test will be performed using the S/C magnetometer.

13. Ground Support System

The SNOE Ground Support System (GSS) will provide the hardware and software needed for instrument and subsystem development, integration, test and pre-launch support. The system architecture is depicted in Figure 18. During the build-up and testing of each instrument and subsystem, three personal computers will be available for acquiring data, controlling equipment, and displaying and analyzing test data. During integration, system testing and pre-launch, two Unix workstations will be used to monitor and control the S/C and to manage and analyze test data. An additional personal computer will be used for flight software development. One of the Unix workstations will reside in the POCC and will be used to conduct and monitor S/C tests. The other Unix workstation will be co-located with the S/C at all times and will connect to the S/C through a test connection or through the communications system to provide test engineers with the information and control that they need.

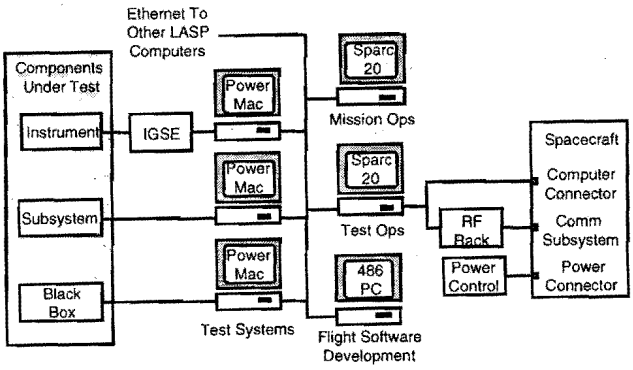

Figure 18. Ground support system architecture

Almost all of the software used in ground testing will be either commercial off-the-shelf (COTS) software or software that LASP has already developed and used on previous projects. This includes the LASP OASIS Command and Control (OASIS-CC) software for monitoring and controlling the S/C and scientific instruments, which is currently used on the Earth Observing System and other NASA projects. The hardware, software and procedures used for ground testing will be re-used during on-orbit operations. This reduces system development cost and makes it much easier to move from the test environment to on-orbit operations. It also permits us to provide student S/C controllers with extensive training by monitoring and controlling the S/C during ground test.

14. Mission Operations

14.1 Tracking and Communications

SNOE ground communications will be handled by a new NASA initiative, the Autonomous Ground Services (AGS). This program has the goal of reducing mission costs through use of small, automated ground stations. The prototype AGS station will be located at Poker Flat, Alaska, and will be backed up by the existing 8-meter Transportable Orbit Tracking Station (TOTS) at that location. AGS antenna sizes will be in the 3–5 meter range; it is anticipated the Poker Flat station will have a 5 meter antenna. S/C communications will use standard NASA S-band protocol. Active tracking and ranging is not provided in the baseline configuration, and so all tracking will be done using NORAD orbit elements and daily predicts. During the orbit injection and acquisition phase, NASA will provide full standard services based out of Wallops Island, which can also be used as a backup in case of problems at Poker Flat.

Command and data relay will be over T1 lines to Goddard Space Flight Center and then to the SNOE POCC at Boulder using either ISDN or T1 service. TCP/IP will be used throughout. This will provide the operations team with real-time access to the S/C during passes and fast acquisition of playback data.

14.2 Mission Operations

S/C and instrument health and safety will be monitored at the POCC located in the LASP Space Technology Research building using the OASIS-CC software package. Flight controllers will also use this software to prepare and transmit commands to the S/C during a pass. Most of the activities during a pass will be coordinated using procedures written in the special CSTOL language that is part of the OASIS-CC software package. Using canned procedures greatly reduces the workload on the controllers. Prior to launch, the student flight controllers and flight engineers will develop and test the CSTOL procedures for both normal and contingency operations of the S/C.

After a pass, all of the data from the S/C will be processed and made available to the flight engineers, who will monitor the long-term health of the satellite and its instruments. Any commands needed to update S/C operations will be prepared by the flight engineers. Because the SNOE is a very simple spacecraft, no special planning and scheduling system is required. Instead, commands will be encoded into CSTOL procedures and transferred to the flight controllers, who will run the procedures to send the commands during a pass. Orbit and attitude determination will be performed by specialists on the flight engineering team.

14.3 Data Processing and Analysis

After each contact with the S/C, real-time and playback data recorded during the contact will be processed. Level 0 processing will be performed to produce the best possible set of packets. Then engineering data will be extracted and checked using the same OASIS-CC software used to assess S/C health during real-time contacts. This will alert mission operations personnel to any anomalies. An updated ephemeris of satellite position will be computed and combined with processed attitude data. The resultant orbit-attitude data—S/C position, velocity and spin vectors, spin reference angle and spin rate—will be stored into the database on one-minute centers.

After the necessary engineering and orbit-attitude have been computed, Level 1 science data processing will be performed. The science team will then analyze the data into higher level data products. All science, engineering and ancillary data products will be stored in a common database. A catalog will be provided so that scientists and engineers can quickly determine which data are available and the quality of the available data. We will provide software for extracting data from the database, interpolating orbit-attitude parameters, and deriving common orbit-attitude parameters needed in science analysis. We will use platform-independent data formats such as HDF or CDF to transfer data to the science team. All data will also be made available over Internet to other investigators.

15. Further Information

For more information on the SNOE project, please visit *http://lasp.colorado.edu/snoe/.*

16. Acknowledgements

Listed as authors on this paper are the Deputy Principal Investigator and graduate students working on the SNOE project at the time the abstract was submitted. However, this is really the work of the entire SNOE team, including the LASP engineering staff, science team, graduate and undergraduate students, USRA, NASA AGS, consultants from Ball Aerospace and elsewhere, and collaborators from JPL, NCAR, the CU Aerospace Engineering department, and Arapahoe High School.

16. References

Barth, C.A., C.W. Hord, J.B. Pearce, K.K. Kelly, G.P. Anderson, and A.I. Stewart, Mariner 6 and 7 UV spectrometer: Upper atmosphere data, *J. Geophys. Res., 76*, 2213, 1971.

Barth, C.A., W.K. Tobiska, D.E. Siskind, and D.D. Cleary, Solar terrestrial coupling: Low-latitude thermospheric NO, *Geophys. Res. Letters, 15*, 92, 1988.

Barth, C.A., Reference models for thermospheric NO, *Adv. Space Res., 10*, 103, 1990.

Barth, C.A., NO in the lower thermosphere, *Planet. Space Sci., 40*, 315, 1992.

Cleary, D.D., Daytime high-latitude rocket observations of NO, *J. Geophys. Res., 91*, 11337, 1986.

Eparvier, F.G. and Barth, C.A., Self-absorption theory applied to rocket measurements of the NO (1,0) γ band in the daytime thermosphere, *J. Geophys. Res., 97*, 13,723, 731, 1992.

Rusch, D.W., G.H. Mount, C.A. Barth, R.J. Thomas, and M.T. Callan, Solar Mesosphere Explorer ultraviolet spectrometer: Measurements of ozone in the 1. to 0.1 mb region, *J. Geophys. Res., 89*, 11677, 1984.

Siskind, D.E., C.A. Barth, and D.D. Cleary, Possible effect of solar soft X-rays on thermospheric NO, *J. Geophys. Res., 95*, 4311, 1990.

Solomon, S., P.J. Crutzen, and R.G. Roble, Photochemical coupling between the thermosphere and lower atmosphere, *J. Geophys. Res., 87*, 7206, 1982.

Solomon, S.C., Auroral electron transport using the Monte Carlo method, *Geophys. Res. Lett., 20*, 185, 1993.

Thomas, G.E. and R.F. Krassa, *Astron. and Astrophys., 11*, 218, 1971.

Woods, T.N., G.J. Rottman, S. Bailey, and S.C. Solomon, Vacuum-ultraviolet instruments for solar irradiance and thermospheric airglow, *Optical Eng., 33*, 438, 1994.